NOVA SCHOOL OF SCIENCE & TECHNOLOGY

DEPARTAMENT OF MATERIALS SCIENCE

ANDRÉ FRUTUOSO ALVES

BSc in Micro and Nanotechnology Engineering

# LOW TEMPERATURE PROCESSING OF DOPED INDIUM OXIDE THIN FILMS FOR ELECTRONIC APPLICATIONS

MASTER IN MICRO AND NANOTECHNOLOGY ENGINEERING

NOVA School of Science and Technology

09, 2023

DEPARTAMENT OF
MATERIALS SCIENCE

# LOW TEMPERATURE PROCESSING OF DOPED INDIUM OXIDE THIN FILMS FOR ELECTRONIC APPLICATIONS

**ANDRÉ FRUTUOSO ALVES**

BSc in Micro and Nanotechnology Engineering

**Adviser:** Rita Maria Mourão Salazar Branquinho
Assistant Professor, NOVA University Lisbon

**Co-advisers:** Emanuel Abreu Antunes Gameiro Carlos
Assistant Researcher, NOVA University Lisbon

**Examination Committee:**

**Chair:** Pedro Miguel Cândido Barquinha,
Associate Professor, NOVA University Lisbon

**Rapporteurs:** Joana Maria Dória Vaz Pinto Morais Sarmento,
Assistant Professor, NOVA University Lisbon

**Adviser:** Emanuel Abreu Antunes Gameiro Carlos,
Assistant Researcher, NOVA University Lisbon

MASTER IN MICRO AND NANOTECHNOLOGY ENGINEERING

NOVA University Lisbon
09, 2023

Low temperature processing of doped indium oxide thin films for electronic applications

Copyright © André Frutuoso Alves, NOVA School of Science and Technology, NOVA University Lisbon.

The NOVA School of Science and Technology and the NOVA University Lisbon have the right, perpetual and without geographical boundaries, to file and publish this dissertation through printed copies reproduced on paper or on digital form, or by any other means known or that may be invented, and to disseminate through scientific repositories and admit its copying and distribution for non-commercial, educational or research purposes, as long as credit is given to the author and editor.

# ABSTRACT

Transparent conducting oxides (TCOs) are critical components in the operation of several optoelectronic devices as well as transparent electronics. One of the most widely used, indium tin oxide (ITO), requires very expensive equipment and controlled conditions to be deposited. Solution combustion synthesis (SCS) is a simple and low-cost method being studied to produce the same oxides. Thin films of indium oxide doped with hafnium produced by SCS have already shown very promising properties when annealed at 400 °C. This work will study the viability of producing these same films at even lower temperatures, enough to enable the use of flexible substrates. TCO thin films were produced at low temperature such as 200 °C by using an infrared (IR) oven instead of the typical hotplate annealing. A 0.5 M % Hf-doped $In_2O_3$ thin film annealed at 350 °C with an IR oven achieved the best properties with a bulk resistivity of $1.3 \times 10^{-1}$ Ω·cm, mobility of 1.33 $cm^2/Vs$, carrier concentration of $3.6 \times 10^{19}$ $cm^{-3}$. These results were even better when compared with high annealing temperatures. As proof of concept this TCO was successfully implemented in a liquid crystal cell and electrochromic device showing their potential for real applications.

**Keywords**: transparent conducting oxide, solution combustion synthesis, indium oxide, hafnium dopant, low temperature, infrared oven.

# RESUMO

Óxidos condutores transparentes (TCOs) são componentes críticos no funcionamento de diversos dispositivos optoeletrónicos bem como eletrónica transparente. Um dos mais usados, óxido de índio e estanho, requer equipamento muito caro e condições controladas para ser depositado. Síntese de solução com combustão (SCS) é um método simples e de baixo custo a ser estudado para produzir os mesmos óxidos. Filmes finos de óxido de índio dopado com háfnio produzido por SCS já mostraram propriedades muito promissoras quando recozidos a 400 °C. Este trabalho irá estudar a viabilidaded the produzir estes mesmos filmes a temperaturas ainda mais baixas, o suficiente para possibilitar o uso de substratos flexíveis. Filmes finos de TCO foram produzidos a temperaturas tais como 200 °C usando um forno de infravermelhos (IR) em vez do típico recozimento numa placa de aquecimento. Um filme fino de $In_2O_3$ dopado com 0.5 M % Hf recozido a 350 °C com um forno de infravermelhos obteve as melhores propriedades com uma resistividade em volume de $1.3 \times 10^{-1}$ Ω·cm, mobilidade de 1.33 $cm^2/Vs$, concentração de portadores de $3.6 \times 10^{19}$ $cm^{-3}$.Estes resultados foram ainda melhores quando comparados com altas temperaturas de recozimento. Como prova de conceito, este TCO foi implementado com sucesso numa célula de cristais líquidos e num dispositivo eletrocrómico mostrando o seu potencial para aplicações reais.

**Palavras chave:** óxido condutor transparente, síntese de solução com combustão, óxido de índio, dopante háfnio, baixa temperatura, forno de infravermelhos.

# CONTENTS

# LIST OF FIGURES

# List of Tables

.

# ACRONYMS

| | |
|---|---|
| **2-ME** | 2-methoxyethanol |
| **DUV** | Deep ultraviolet |
| **EFD** | Extremely fuel deficient |
| **EFE** | Extremely fuel excess |
| **EG** | Ethylene Glycol |
| **FD** | Fuel deficient |
| **FE** | Fuel excess |
| **IC** | Integrated circuit |
| **IGZO** | Indium Gallium Zinc Oxide |
| **IR** | Infrared |
| **ITO** | Indium Tin Oxide |
| **IZO** | Indium Zinc Oxide |
| **LCD** | Liquid Crystal Display |
| **M%** | Molar percentage |
| **MP** | 1-methoxy-2-propanol |
| **PTFE** | Polytetrafluoroethylene |
| **PVA** | Polyvinyl alcohol |
| **rpm** | Rotations per minute |

| | |
|---|---|
| **SCS** | Solution Combustion Synthesis |
| **TCO** | Transparent conducting oxide |
| **UV** | Ultraviolet |

# SYMBOLS

| | |
|---|---|
| N | Carrier concentration |
| $T_{380-750nm}$ | Transmittance in the visible range of the spectrum |
| $\varrho$ | Resistivity |
| $\mu$ | Carrier mobility |

# Motivation and Objectives

Transparent conducting oxides (TCOs) are critical components in the operation of several optoelectronic devices as well as transparent electronics. One of the most widely used, indium tin oxide (ITO), requires very expensive equipment and controlled conditions such as high vacuum and noble gases to be deposited. Solution combustion synthesis (SCS) is a simple and low-cost method being studied to produce the same oxides.

Indium oxide doped with hafnium thin films produced by SCS have already shown very promising properties when annealed at 400 °C (bulk resistivity of $5.73 \times 10^{-2}$ Ω·cm, mobility of 6.65 $cm^2/Vs$) [1]. With this work we hope to show the viability of SCS to produce doped indium oxide thin films at even lower temperatures for applications that do not require a TCO as conductive as commercial ITO or other films annealed at higher temperatures. This would not only save energy by using a lower temperature but also allow more commonplace equipment to be able to produce TCOs, reducing the barrier of entry to anyone wanting to produce TCOs. The lower temperatures would also hopefully allow the use of flexible substrates and other depositions methods.

The main objectives of this are:

- Test various types of annealing methods on $In_2O_3$ thin films to determine the most suitable one.
- Test the difference between solvents on the films' properties, including environmentally friendly ones.
- Use 400 °C and lower annealing temperatures and characterize the films' optical, electrical and structural properties.
- Implement these films on devices to assess their viability.

# 1 INTRODUCTION

## 1.1 Transparent conducting oxides

Transparent conducting oxides (TCOs) are known as such for presenting both low resistivity ($\rho \sim 10^{-4}$ Ω·cm) and high transmittance in the visible range ($T_{380–750nm} > 80\%$) which requires a bandgap above 3 eV [2]–[4]. TCOs are conducting oxides whose conductivity is due to doping either by oxygen vacancies or extrinsic dopants that help populate the conduction band [2]. The doping amount must, however, be carefully analyzed because too high of a doping concentration can reduce the carrier mobility to a point where the conductivity stops improving [2]. The most popular dopants vary depending on the TCO but the most popular for $In_2O_3$ are Sn, Mo, Ta, W, Zr, F, Ge, Nb, Hf and Mg [2].

Nowadays, the most widely used TCO is indium tin oxide (ITO). Indium oxide will also be used in this work but doped with hafnium or zirconium instead of tin. TCOs are especially important in the areas of transparent electronics and optoelectronics, in applications like solar cells, displays and transparent thin film transistors and others shown in **Figure 1.1.** [2], [5], [6].

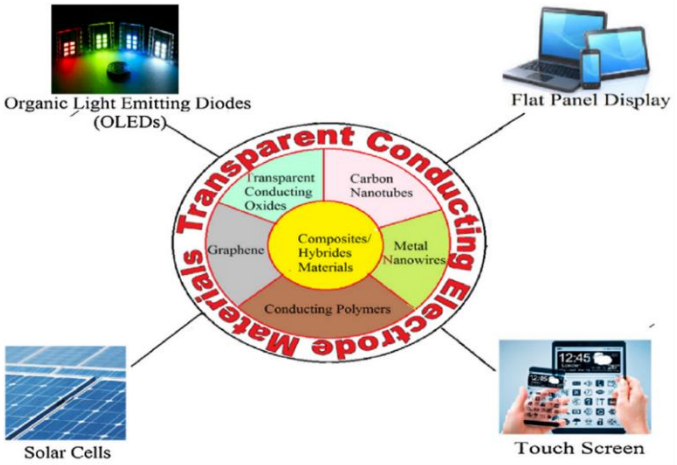


**Figure 1.1.** Transparent Conducting Electrode Materials and their applications [6].

In, for example, liquid crystal displays (LCDs), TCOs act as the electrodes that allow the various lines and columns to be addressed as well as allowing the light from one side, after being manipulated by the liquid crystals, to be visible on the other side, ultimately allowing the display to show what we want it to show [7]. (Pixel switching).

In an electrochromic device, TCOs are used again as an electrode because this allows the device to appear transparent, when not colored, and once the coloring is desired it allows voltage to flow to the electrochromic material to cause a color change [8].

## 1.2 Solution combustion synthesis

Solution combustion synthesis (SCS) can be used to produce simple and complex oxides with a desired size and shape by changing parameters like fuel type, metal cations precursors, stoichiometry ratio, pH, atmosphere and initiation type [9].

As the name suggests, being a combustion, there are three main components needed for the synthesis reaction to occur, a fuel that will be oxidized during the reaction, usually composed by organics containing carbon and hydrogen, an oxidizer that will be reduced, usually metal nitrates, and a temperature high enough to start the reaction [9].

SCS is a specific type of the broader self-propagating high-temperature synthesis (SHS), distinguishing itself through three features. The first is that the initial components are mixed in aqueous solution at the molecular level, the second is that the reaction responsible for the solid product formation in SCS can be different from the self-sustained combustion process. Thirdly, the SCS process generates a large amount of gaseous byproducts which leads to an expansion of the solid product, and a fast decrease in temperature after the reaction, making the solid product porous and finely dispersed, critical features in SCS of nanoscale powders [10].

There are also three main stages during an SCS process, the combustion mixture formation, the gel formation, and the combustion of the gel as can be seen from **Figure 1.2.** Simplified scheme of the SCS process [12]. [9], [11], [12].

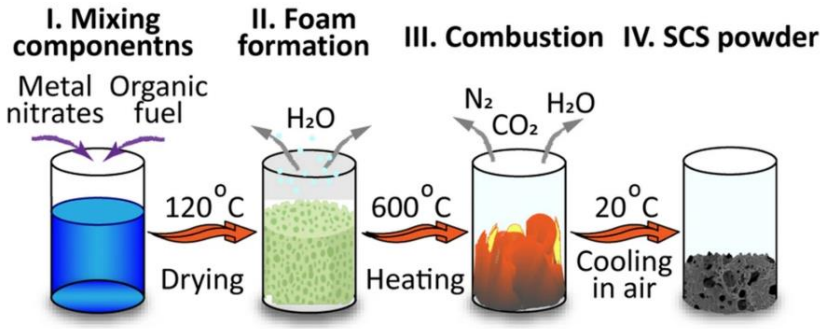


**Figure 1.2.** Simplified scheme of the SCS process [12].

The choice of the fuel used in SCS is very important because it has many different functions. It is a reducer, a chelating agent, being able to interact with the metal cations to form the gel network and acts as the microstructural template for the final product. Through the use of different fuels and fuel amounts, it is possible to change the structure, the microstructure-morphology, texture, surface, redox-catalytic behavior and conductivity of materials [13].

The metal cation precursors mainly have the role of providing metal cations, determining the final metal oxide. Different metal cations also present different decomposition temperatures, inversely proportional to the charge density, which affects the processing conditions to form different morphologies [1].

The fuel to oxidizer ratio can be divided in 5 different categories: extremely fuel deficient (EFD) which requires external heating and leads to a massive evolution of gases, fuel deficient (FD) which leads to a slow reaction also requiring external heating, the stoichiometric combustion generates the most heat possible and achieves a maximum combustion efficiency, the fuel excess (FE) and extremely fuel excess (EFE) can lead to a higher amount of impurities in the final product [9].

The pH of the solution also has a noticeable effect. The main one is the effect it will have on the chelation ability to the metal cations. Keeping the pH slightly acidic will also avoid the formation of metal hydroxides as well as other salts. It can also have some effects on the intensity of the reaction and the structure morphology of the final oxide [9], [11].

The last parameters that affect the oxides produced are the atmosphere environment and initiation type. Though the atmosphere environment effects have not been thoroughly explored, it has been noticed that in a flowing air environment a faster reaction process occurs as opposed to a nitrogen environment, but in the nitrogen environment there is an improved mass-changing rate in SCS. The most popular initiation type is the muffle furnace for providing uniform heating leading to a violent combustion reaction. Mainly for the production of thin films, hotplate annealing has been frequently used as initiation type. Lastly, a mi-

crowave heating source has been shown to result in better microstructural and textural properties. Though this heating method presents limitations due to the high cost of the equipment and low scalability [9], [11].

Through the change in all these different parameters, SCS allows for the synthesis of not only thin films but also various nanostructures such as nanobelts, nanoflakes, nanoflowers, nanoneedles, nanosheets, nanoplates, nanorods, nanowires, nanopowders and nanoparticles [9].

When compared to the conventional sol-gel technique, SCS has shown its viability to produce metal oxide thin films at a much-reduced temperature, opening the window for different electronic applications [9].

ITO requires very expensive equipment to be deposited. SCS is showing promising results to produce high quality oxide thin films while not requiring expensive high vacuum equipment.

## 1.3 Annealing method

There have been various different annealing methods for thin films produced with SCS, ranging from methods that don't have cumbersome limitations (chamber, controlled environment, substrate type)[14] like the basic hotplate or UV irradiation to the ones that do have them like microwave irradiation annealing, rapid thermal annealing, high-pressure annealing, atmospheric-pressure plasma, and plasma-assisted annealing [15]–[20].

UV irradiation, especially deep-ultraviolet (DUV) has been shown to produce efficient condensation and densification of oxide semiconductor films (IGZO and IZO) at temperatures as low as 150 °C [21]. The films' quality and densification were then improved further by combining this UV irradiation with SCS for thin-film transistor applications, one of these results can be seen in **Figure 1.3.** [9], [22]–[24]. This combination also allowed *Fortunato et al.* to, for the first time, perform flexographic printing of a highly-stable aluminum-oxide dielectric with a high-throughput (50 m/min) while simultaneously demonstrating low-temperature processing (≤ 200 °C) [25].

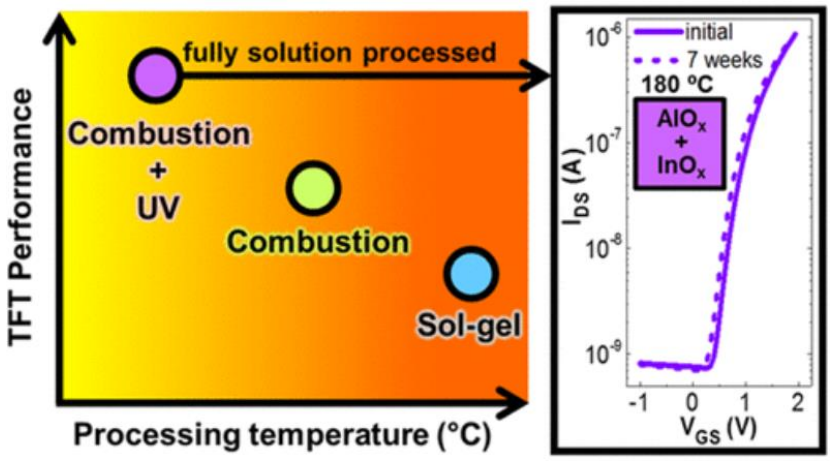


**Figure 1.3.** Proposed mechanism of the low temperature photoactivation combined with the combustion synthesis of metal oxide thin films for TFT performance [9].

As discussed, the combination between SCS and UV irradiation has shown to be incredibly promising to produce TCOs with low cost, low temperature and with potential for scalability and so it will also be tested in this work. Although this does not mean that other annealing methods are not worth investigating as well, which will be done in this work.

# 2
# MATERIALS AND METHODS

In this section, the various reagents and the methods used to produce the various solutions used in this work are introduced. The deposition as well as the various characterization methods used are also explained. Lastly, the way of producing both applications for the films created is presented.

## 2.1 Precursor solutions preparation

Four different 0.2 M concentration metal cation precursor solutions were prepared by dissolving indium (III) nitrate hydrate ($In(NO_3)_3 \cdot xH_2O$, Sigma, 99.9 %, CAS 207398-97-8) in 10 mL of solvents which were 2-methoxyethanol (2-ME, $C_3H_8O_2$, Alfa Aesar, 99 %, CAS 109-86-4) for two solutions; 1-methoxy-2-propanol (MP, $C_4H_{10}O_2$, Roth, $\geqslant$ 99 %, CAS 107-98-2) for one solution; and ethanol absolute anhydrous ($C_2H_6O$, Carlo Ebra, $\geqslant$ 99.9 %, CAS 64-17-5) and ethylene glycol (EG, $C_2H_6O_2$, Carlo Erba, $\geqslant$ 99.5 %, CAS 107-21-1) at a proportion of 4:1 for the final solution. As a fuel for the combustion, urea ($CH_4N_2O$, Sigma, 99.0-100.5 %, CAS 57-13-6) was used in all solutions except for the ethanol and EG solution since the EG already acts as fuel. To guarantee the redox stoichiometry of the reaction, a molar ratio of 2.5:1 was used for the urea and indium nitrate respectively [1].

As dopant sources, to one of the 2-ME solutions, 1 M% of zirconium (IV) oxynitrate hydrate ($ZrO(NO_3)_2 \cdot xH_2O$, Sigma, 99 %, CAS 14985-18-3) was added and 0.5 M% of hafnium (IV) chloride ($HfCl_4$, Alfa Easer, 99.9 %, CAS 13499-05-3) was added to all the remaining solutions [1].

All solutions were then stirred at 430 rpm at room temperature for at least 1 hour to guarantee proper dissolution of all the reagents.

## 2.2 Thin film deposition and characterization

The films were deposited on both corning glass and p-type silicon wafer substrates with an area of 2.5 × 2.5 $cm^2$. Prior to the deposition, the substrates were cleaned in an ultrasonic bath at 60 °C in acetone for 15 minutes, then in 2-isopropanol for 15 minutes and dried under $N_2$. UV/Ozone surface activation was also performed for 15 minutes using a PSD-UV Novascan system.

For each thin film, 8 layers of a solution, filtered through 0.45 μm hydrophobic polytetrafluoroethylene (PTFE) filters, were deposited by spin coating for 35 s at 3000 rpm with an acceleration of 2000 rpm (Laurell Technologies). After each layer was deposited, a 5 minute annealing was performed and after all 8 layers an annealing of 2 hours was performed. Different annealing temperatures (200 °C; 250 °C; 300 °C; 350 °C) and methods (hotplate, UV and an ECO-WORTHY T-962 infrared IC oven) were used to determine their influence on the thin film's properties.

The thickness of the films deposited on silicon wafers was determined by spectroscopic ellipsometry, made over an energy range of 1.5–5 eV with an incident angle of 70° using a Jobin Yvon Uvisel system. The acquired data was modulated using the DELTAPSI software, and the fitting procedure was done pursuing the minimization of the error function ($\chi^2$).

The optical properties, particularly the transmittance, were obtained using a Shimadzu UV-3101PC UV/VIS/NIR spectrophotometer from 200 to 3000 nm.

After the deposition of aluminum contacts by thermal evaporation, the electrical properties were obtained by Hall effect measurements (Biorad HL5500) using a Van der Pauw geometry at a constant magnetic field of 0.5 T at room temperature, with 2 cycles and a delay time and integration time of 3 seconds.

The structural analysis of the films deposited on silicon wafers was made using data obtained by X-ray diffraction (XRD) using a PANalytical MPD X'Pert PRO powder diffractometer, with a Cu Kα radiation source (λ = 1.540598 Å) and equipped with a 1D X'Celerator detector. The XRD measurements were performed in the range of 10 to 65° (2θ) in the Bragg-Brentano configuration, with a scanning step size of 0.0334° in 2θ.

## 2.3 Liquid crystal cell production

To make the liquid crystal cell, PVA (MW 20000-30000, CAS 9002-89-5) was deposited via spin-coating (30 s @ 1500 rpm) onto two pieces of glass with unpatterned solution-based

indium oxide thin film already deposited. Rubbing was then performed to create grooves to align the liquid crystal molecules. The two pieces of glass were then glued together with the grooves at a 90° orientation. Finally, the liquid crystal 4-cyano-4'-pentylbiphenyl (5CB) filled the gap between the glasses through capillarity. The liquid crystal cell was modulated by applying voltage between the two TCO electrodes.

## 2.4 Electrochromic device production

To make the electrochromic device, a thin film of tungsten(VI) oxide ($WO_3$), also prepared via SCS, was deposited using spin-coating on a glass with the solution-based indium oxide thin film already deposited. The electrochromic cell was tested using LiClO4/PC electrolyte and by applying voltage to perform colouring and bleaching cycles.

# 3
# RESULTS AND DISCUSSION

This section will explain how the parameters used to produce the best films were determined. Films with these parameters will then be annealed at 4 different temperatures (200 °C; 250 °C; 300 °C; 350 °C) and will undergo various characterization techniques. Finally, two proof of concept applications will be shown to prove the films' viability.

## 3.1 Determining the best parameters to use

In a previous master thesis [1], it was already shown that the best properties were achieved for doped indium oxide TCOs when 0.2 M solution concentration and 8 layers are used. Considering this, all solutions and thin films were made with these. That master thesis also determined the best dopant concentration for indium oxide thin films, 0.5 M% Hf and 1 M% Zr.

In this work the tests were performed to determine the best dopant, annealing method, annealing time, and solvent to use.

### 3.1.1 Dopant

As mentioned, in a previous master thesis [1], the best dopants and their concentration were found to be 0.5 M% Hf and 1 M% Zr. The initial intention was to use both dopants for every condition tested but as a measure to be able to test the greatest number of conditions possible, after testing a few different conditions with both dopants, the one that showed the best properties was chosen as the sole one to be used in all other conditions.

Three films with different conditions (1h - Hotplate - 400 °C; 2h - IR - 350 °C; 2h - IR - 300 °C), but all with 2-ME as the solvent, and both dopants were tested, and the properties are presented in **Table 3.1**. Additionally, the $T_{380\text{-}750nm}$ the films can be observed in annex **Table A.3**; **Table A.4**; **Table A.5**.

While in one of the films (1h - Hotplate - 400 °C), Zr-$In_2O_3$ presents a slightly lower resistivity than Hf-$In_2O_3$, on the other two it is the opposite and there is even a large difference in one of them. Considering this and the fact that Zr-$In_2O_3$ always has a lower mobility than Hf-$In_2O_3$, Hf was chosen as the dopant to be used in all the films produced in this work.

**Table 3.1.** Thickness obtained by spectroscopic ellipsometry and electrical properties by Hall effect measurements of three indium oxide thin films with different conditions (time, type and temperature of annealing) and both dopants.

| Film conditions | Dopant | Thickness (nm) | ϱ (Ω·cm) | μ ($cm^2/V·s$) | N ($\times 10^{19}$ $cm^{-3}$) |
|---|---|---|---|---|---|
| 1h - Hotplate - 400 °C | Hf | 85.8 ± 0.8 | 0.59 ± 0.14 | 1.95 ± 0.4 | 0.56 ± 0.02 |
| | Zr | 83.2 ± 0.6 | 0.31 ± 0.18 | 1.3 ± 0.34 | 0.71 ± 0.22 |
| 2h - IR - 350 °C | Hf | 87.1 ± 0.9 | 0.13 ± 0.01 | 1.33 ± 0.06 | 3.6 ± 0.2 |
| | Zr | 87.8 ± 0.8 | 0.18 ± 0.07 | 1.13 ± 0.29 | 1.3 ± 0.3 |
| 2h - IR - 300 °C | Hf | 96.1 ± 1 | 1.42 ± 0.24 | 0.86 ± 0.05 | 0.53 ± 0.09 |
| | Zr | 95 ± 0.4 | 9.37 ± 3.32 | 0.44 ± 0.16 | 0.07 ± 0.01 |

### 3.1.2 Annealing method

A common equipment to perform annealing, especially in a lab environment, is a hotplate. To determine if other equipment can achieve better properties at the same temperature or even at lower temperatures, an infrared oven as well as the heating capabilities of the PSD-UV Novascan system were used.

The three different methods were used to perform annealing on films with the same properties, the only difference being that the annealing with hotplate + UV was only done for 1 hour while the other two were performed for 2 hours, all at 300 °C. The detailed film conditions and properties can be found in annex **Table A.1**.

**Figure 3.1.** shows that the film annealed with the IR oven presents the lowest resistivity, but on the films annealed with the hotplate it is only slightly higher, whereas the film annealed with the help of the UV shows a massive increase in resistivity, about four orders of magnitude. This leads us to believe that the combustion reaction was not properly activated using this method, which can be corroborated by the low intensity of the peaks in the XRD data which indicates low crystallinity of the film annealed by this method as opposed to the other two. Because of this result, all the films in this work after this section were only made using the IR oven and the hotplate annealing.

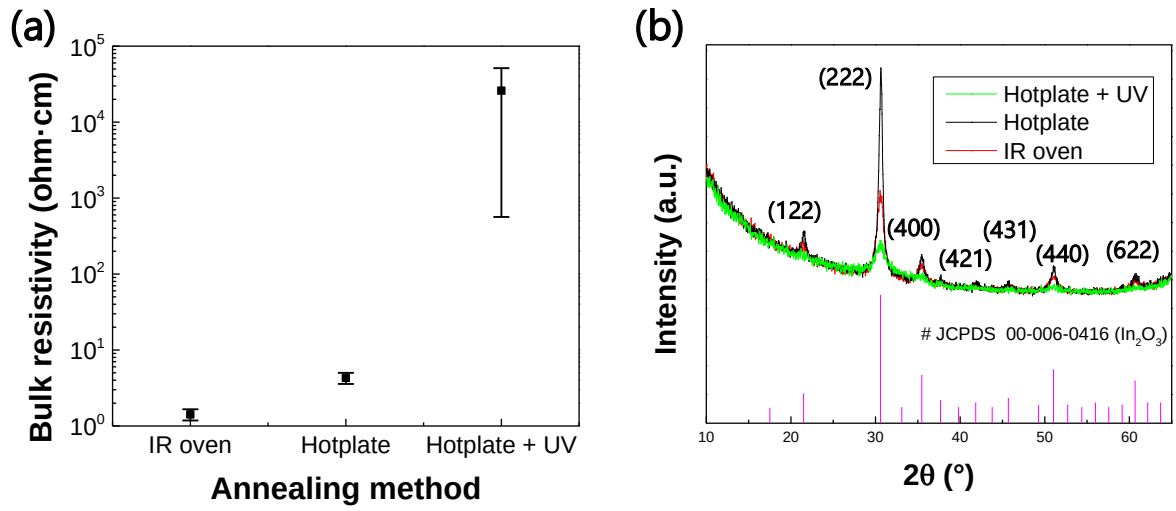


**Figure 3.1. (a)** Bulk resistivity obtained via Hall effect measurements and **(b)** XRD of the same Hf-doped indium oxide thin film annealed using different methods at 300 °C.

### 3.1.3 Annealing time

In the aforementioned master thesis [1], 1 hour of annealing was used after all the layers were deposited. To determine if this is in fact the best post-annealing time condition, the comparison between the same film with 1 hour and 2 hours of annealing as well as between 2 hours and 4 hours was done, all performed in an IR oven. The results are shown in **Figure 3.2.** where it can be seen a decrease in resistivity when annealing the thin films for 2 h compared to just 1 h. Also, an increase is observed in resistivity when going as far as 4 hours, this is due to the deterioration of the film as it is heated for longer periods of time [26]. With these results it was decided to perform 2 hours of annealing in every film from now on. The detailed film conditions and properties can be found in annex **Table A.2**.

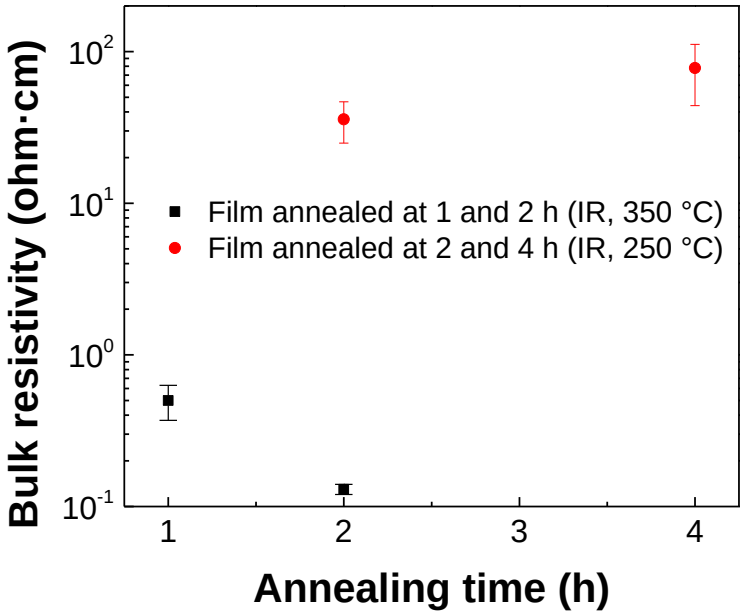


**Figure 3.2.** Bulk resistivity of Hf-doped indium oxide thin films annealed in an IR oven for different durations.

### 3.1.4 Solvent

One of the most used solvents in the fabrication of oxide thin films, 2-ME was compared to more environmentally friendly alternatives such as MP and ethanol to assess if these could have similar properties. The test was done by performing the exact same process in all three films apart from changing the solvent used in the solutions. The detailed film conditions and more properties can be found in annex **Table A.6**.

In **Table 3.2** the electrical properties as well as the thickness of these films are presented. From these results it can be seen that the film with the lowest resistivity (0.13 ± 0.01 Ω·cm) is produced with 2-ME but, while films produced with MP has a slightly higher resistivity (0.31 ± 0.01 Ω·cm), the mobility is significantly higher. When ethanol + EG solvent is used, the film shows both higher resistivity and lower mobility when compared with both other solvents, and for these reasons, going forward the films were produced with both MP and 2-ME.

**Table 3.2.** Thickness obtained by spectroscopic ellipsometry and electrical properties by Hall effect measurements of three Hf-doped indium oxide thin films whose only difference was the solvent used.

| Solvent | Thickness (nm) | ϱ (Ω·cm) | μ ($cm^2/V·s$) | N ($\times 10^{19}$ $cm^{-3}$) |
|---|---|---|---|---|
| 2-ME | 87.1 | 0.13 ± 0.01 | 1.33 ± 0.06 | 3.6 ± 0.2 |
| MP | 125.2 ± 0.9 | 0.31 ± 0.01 | 4.02 ± 0.59 | 0.5 ± 0.1 |
| Ethanol + EG | 117.4 ± 0.6 | 0.74 ± 0.12 | 0.39 ± 0.18 | 2.4 ± 0.7 |

## 3.2 Annealing temperature effect on Hf-$In_2O_3$ films

With the various parameters defined, an annealing for 2 hours was performed at four temperatures (200 °C; 250 °C; 300 °C; 350 °C) using a hotplate and an IR oven as well as using solutions with 2-ME and MP solvents and both of these solutions using 0.5 M% Hf doping. Thus, producing a total of 16 different samples whose properties were measured and compared.

### 3.2.1 Thickness

The thickness of the various films was measured and are presented in **Figure 3.3.** These results show, with only a couple outliers, a clear trend for the thickness to increase as the annealing temperature decreases. This result is expected as the higher temperatures lead to a higher densification of the film, leading to thin films thickness reduction. Also, we can see a fairly constant difference between the thickness of the films made with different solvents.

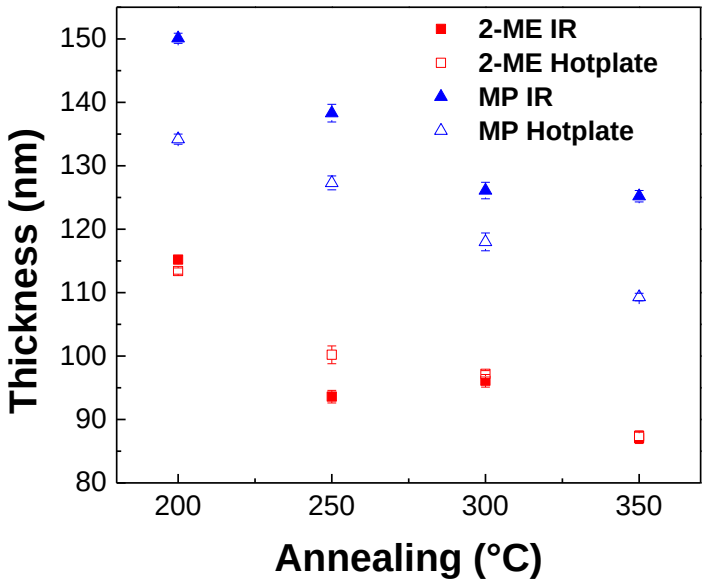


**Figure 3.3.** Thickness of various Hf-doped indium oxide thin films annealed at four different temperatures.

### 3.2.2 Structural characterization

Using the data obtained from XRD measurements, the crystallinity of each combination of solvent and annealing method was compared for each of the four temperatures, as shown in **Figure 3.4.** it can be observed that in every condition, except for one film (MP, hotplate, 300 °C), the films get less crystalline as the annealing temperature decreases, this could be due to the lower temperatures not being able to fully start the combustion reaction. Also, the level of crystallinity increases with higher annealing temperatures due to lattice relaxation [11]. Besides this, a higher crystallinity and bigger crystallite size at the same temperatures is observed in the thin films when annealing with a hotplate compared to the IR oven.

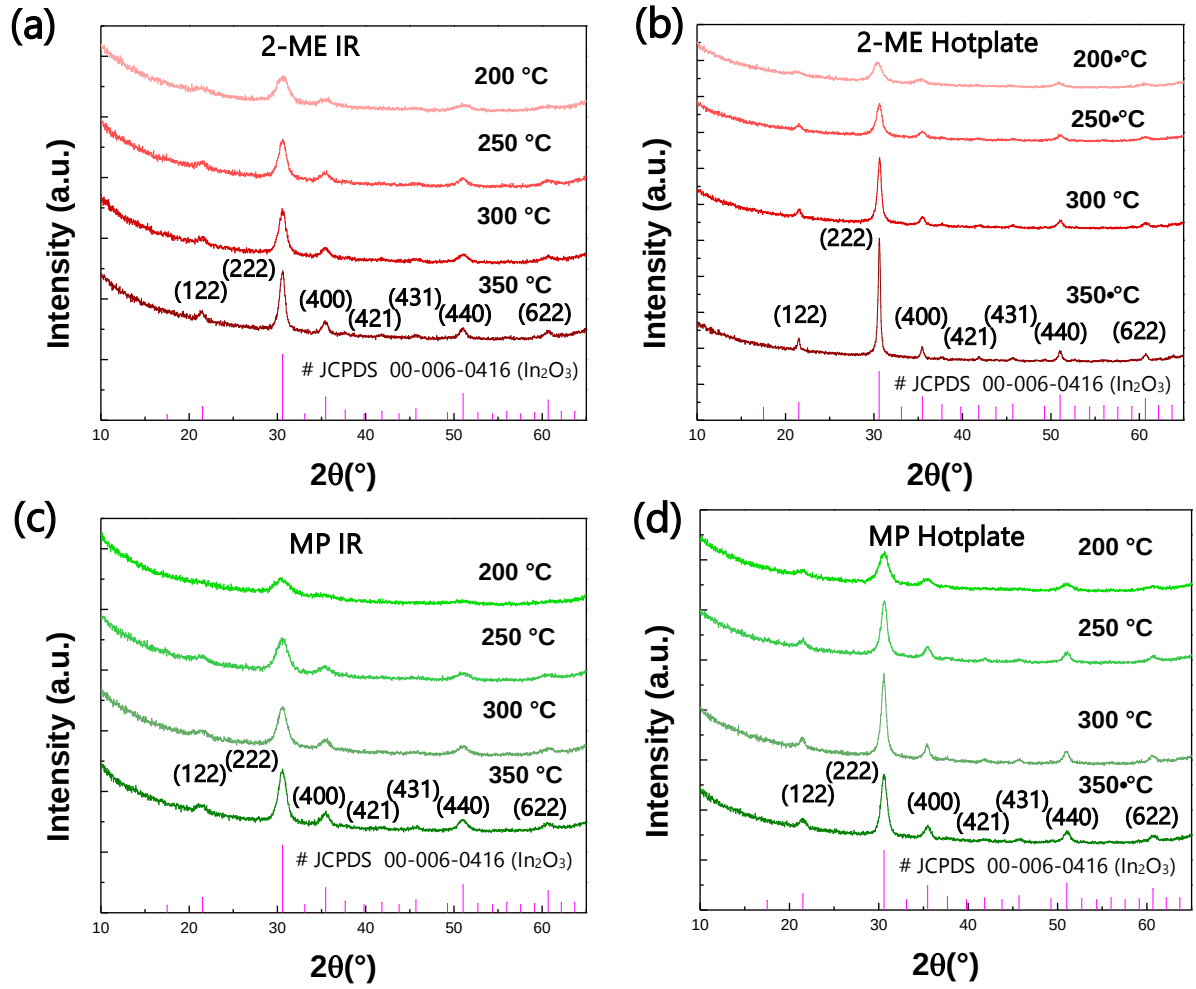


**Figure 3.4.** XRD measurements of four films between 200 and 350 °C whose solvent and annealing method were 2-ME **(a)** IR oven, **(b)** hotplate and MP **(c)** IR oven, **(d)** hotplate.

### 3.2.3 Optical characterization

The average transmittance in the visible range of the spectrum of all the films can be seen in **Table 3.3**, showing, in both solvents and annealing methods, a decrease in transmittance as the annealing temperature increases. This goes in the opposite direction when compared with the crystallinity, resistivity and carrier concentration results presented in the next section. There is also always, for the same temperature, a higher transmittance when annealing with a hotplate compared to the IR oven which again goes opposite to the crystallinity of the films. As for the solvents, MP presents a higher transmittance than 2-ME for every condi-

tion. Despite the lowering transmittance with the higher temperatures, all the films still show a transmittance in the visible spectrum higher than 80 %. The transmittance spectra can be seen in annex C.

**Table 3.3.** Transmittance on the visible range of Hf-doped indium oxide thin films made with two different solvents and annealed by two different conditions hotplate and IR oven from 200 °C to 350 °C.

| Annealing conditions | $T_{380\text{-}750nm}$ (%) | | | |
|---|---|---|---|---|
| | 2-ME | | MP | |
| | Hotplate | IR | Hotplate | IR |
| 200 °C | 89 ± 2 | 85 ± 3 | 90 ± 4 | 88 ± 3 |
| 250 °C | 86 ± 3 | 84 ± 2 | 88 ± 3 | 87 ± 3 |
| 300 °C | 85 ± 3 | 82 ± 2 | 88 ± 3 | 86 ± 4 |
| 350 °C | 82 ± 2 | 81 ± 2 | 86 ± 4 | 84 ± 4 |

### 3.2.4 Electrical characterization

The electrical properties are an average of three measurements for each film and the various results are presented in four graphs in **Figure 3.5.** with the films identified as solvent+annealing method. The full properties of the films can be consulted in annex B. As a side note, due to the films that were annealed at 200 °C having very high resistivities and low mobilities, there were some difficulties acquiring the electrical properties for these films. This was due to them being at the limit of what the hall effect system used was capable of measuring and thus, these results should not be trusted.

As expected, the resistivity is inversely proportional to the carrier concentration since conductivity is proportional to carrier concentration. The bulk resistivity shows a fairly consistent difference between temperatures, especially when annealed with IR, of about an order of magnitude. In general, the mobility increases with annealing temperature and, with one exception, all the films at 300 and 350 °C are extremely close to each other.

We can see that the film with the lowest resistivity is the one annealed at 350 °C using the IR oven with 2-ME as the solvent.

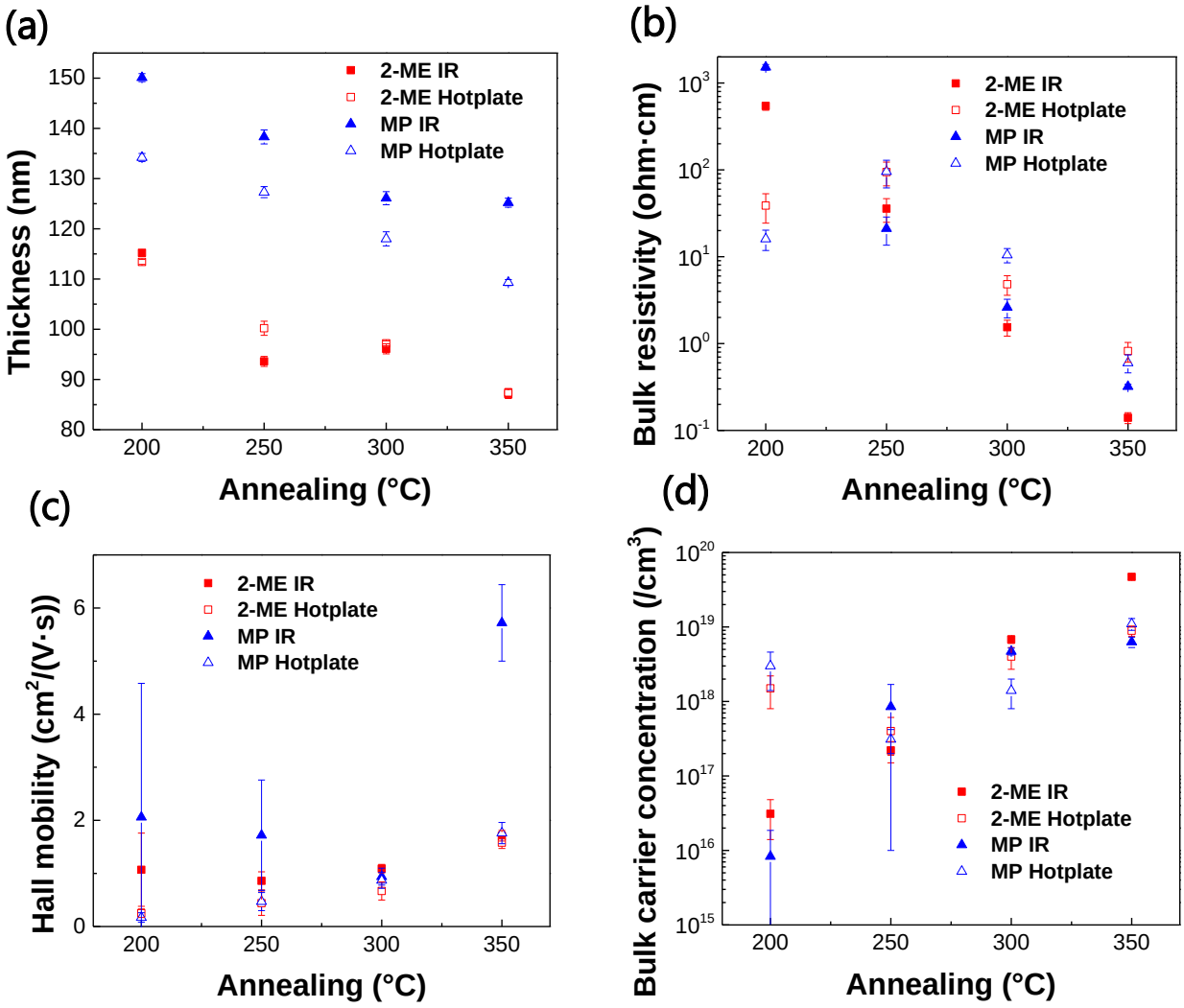


**Figure 3.5.** **(a)** Thickness and electrical properties by Hall effect measurements such as **(b)** bulk resistivity, **(c)** Hall mobility and **(d)** bulk carrier concentration of various Hf-doped indium oxide thin films annealed at four different temperatures.

## 3.3 Proof of concept applications

As a way to show the viable use of solution-based doped indium oxide thin films annealed at temperatures as low as 350 °C, the film with the best electrical properties (2-ME solvent, Hf doping, annealed with IR oven for 2 hours) was used as an electrode in two devices, a liquid crystal cell and an electrochromic cell, instead of the standard commercial ITO.

### 3.3.1 Liquid crystal cell

The result of a test of the liquid crystal cell in a normally white configuration using a 9 V battery is presented in **Figure 3.6.** It is clearly visible that the cell goes from transparent to opaque with the applied voltage, indicating the proper functioning of the cell and showing that this film is viable for this type of application.

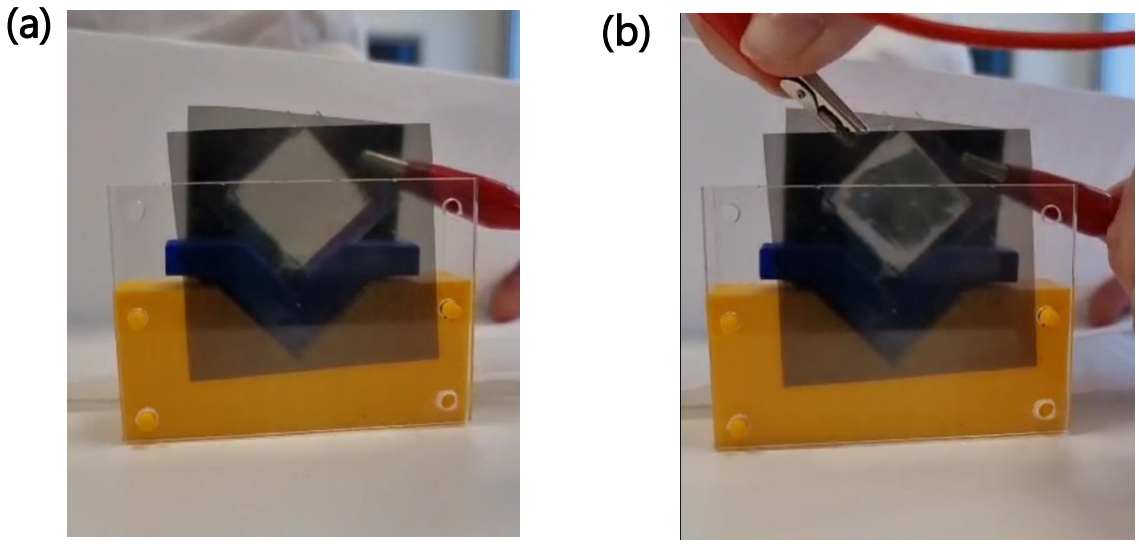


**Figure 3.6.** Liquid crystal cell in normally white configuration. **(a)** before applied voltage, **(b)** after applied voltage.

### 3.3.2 Electrochromic device

This TCO was also implemented as bottom electrode for electrochromic devices based on $WO_3$ as the active layer. The before and after applying voltage to the TCO can be seen in **Figure 3.7.** There is a strong blue coloration, typical from $WO_3$, after the applied voltage [27], showing that the device is working properly and again showing that this film is viable for this application. The difference between using this film and the commercial ITO was in the voltage required for the coloring to occur. The commercial ITO colored between 3 and 4.5 V

while this film colored between 9 and 13 V, which is due to the higher resistivity when compared to the commercial ITO.

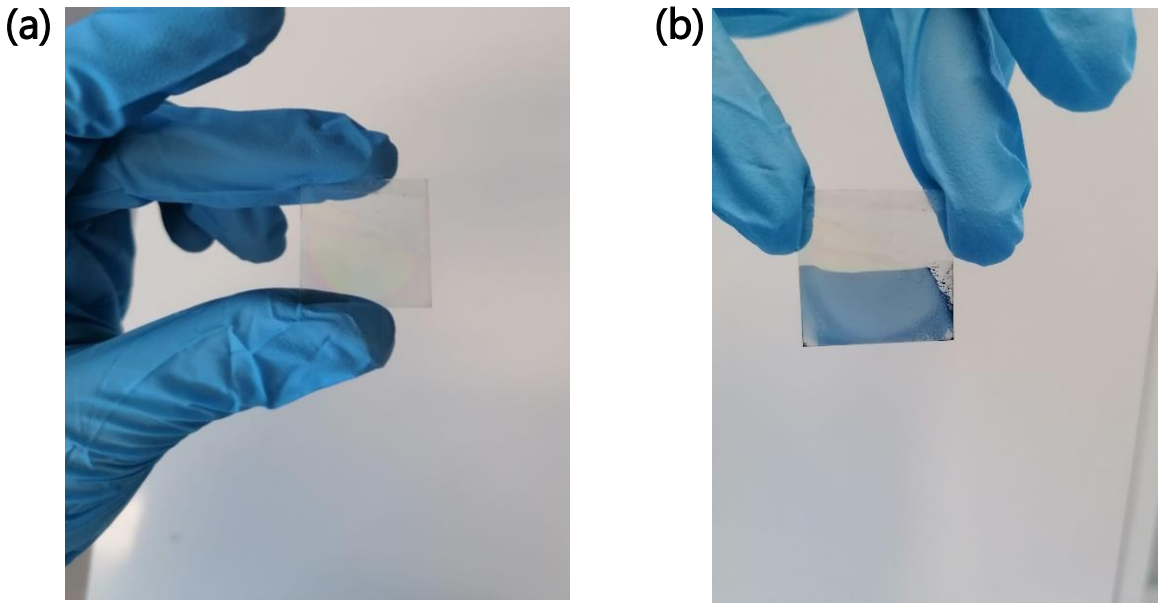


**Figure 3.7.** Electrochromic device **(a)** before applied voltage, **(b)** after applied voltage.

# 4

# Conclusions and Future Perspectives

The goal of showing the viability of SCS to produce thin films at temperatures lower than 400 °C was achieved by successfully using a film annealed at 350 °C in two applications that showed the same behavior as when using commercial ITO as the TCO.

Various properties were accessed and tested to find the best ones when producing hf-doped indium oxide when using SCS such as IR oven and hotplate being the best annealing methods, the best annealing time being 2 hours, the best dopant between Zr and Hf being Hf, and the best solvents being 2-ME and MP.

After defining these parameters, 16 films varying the solvent and annealing method were produced to find the influence of annealing temperature on various of the films' properties such as thickness, showing that it decreases with higher temperatures, crystallinity which increases with higher temperatures, transmittance, especially the transmittance in the visible spectrum which decreases with higher temperatures but all films were still higher than 80 %, and finally the electrical properties of which the bulk resistivity decreases with temperature, inversely, bulk carrier concentration increases with temperature and Hall mobility generally increases with temperature.

Overall, the viability of SCS to produce TCOs at low temperatures with usable properties was proven as well as an IR oven achieving overall better TCO properties than a hotplate which can be beneficial if there is ever an attempt to produce these films at a larger scale since these are the types of ovens usually used in industrial settings.

In the future there are various different directions where the tests for these films can go, including testing flexible substrates of which a test with XENOMAX was done during this work but due to various problems during the deposition process, these did not present usable properties.

Studies can also be done to try to use different deposition methods such as roll-to-roll or inkjet printing, methods which would reduce the waste of material that occurs when doing spin-coating.

The tests in applications can also be taken further such as using films annealed at lower temperatures to produce liquid crystal cells as well as testing the chemical erosion of these films to be able to produce patterned cells.

# 5
# REFERENCES


[1] R. Firmino, "Solution Processing of Doped Indium Oxide for Applications as Transparent Conducting Oxides," MsC thesis, NOVA University Lisbon, 2021.

[2] R. A. Afre, N. Sharma, M. Sharon, and M. Sharon, "Transparent Conducting Oxide Films for Various Applications: A Review," *REVIEWS ON ADVANCED MATERIALS SCIENCE*, vol. 53, no. 1, pp. 79–89, Jan. 2018, doi: 10.1515/rams-2018-0006.

[3] T. Minami, "Transparent conducting oxide semiconductors for transparent electrodes," *Semicond Sci Technol*, vol. 20, no. 4, pp. S35–S44, Apr. 2005, doi: 10.1088/0268-1242/20/4/004.

[4] G. T. Chavan *et al.*, "A Brief Review of Transparent Conducting Oxides (TCO): The Influence of Different Deposition Techniques on the Efficiency of Solar Cells," *Nanomaterials*, vol. 13, no. 7, p. 1226, Mar. 2023, doi: 10.3390/nano13071226.

[5] A. Stadler, "Transparent Conducting Oxides—An Up-To-Date Overview," *Materials*, vol. 5, no. 12, pp. 661–683, Apr. 2012, doi: 10.3390/ma5040661.

[6] S. Sharma, S. Shriwastava, S. Kumar, K. Bhatt, and C. C. Tripathi, "Alternative transparent conducting electrode materials for flexible optoelectronic devices," *Opto-Electronics Review*, vol. 26, no. 3, pp. 223–235, Sep. 2018, doi: 10.1016/j.opelre.2018.06.004.

[7] T. Minami, "Substitution of transparent conducting oxide thin films for indium tin oxide transparent electrode applications," *Thin Solid Films*, vol. 516, no. 7, pp. 1314–1321, Feb. 2008, doi: 10.1016/j.tsf.2007.03.082.

[8] P. Talvenmaa, "Introduction to chromic materials," in *Intelligent Textiles and Clothing*, Elsevier, 2006, pp. 193–205. doi: 10.1533/9781845691622.3.193.

[9] E. Carlos, R. Martins, E. Fortunato, and R. Branquinho, "Solution Combustion Synthesis: Towards a Sustainable Approach for Metal Oxides," *Chemistry – A European Journal*, vol. 26, no. 42, pp. 9099–9125, Jul. 2020, doi: 10.1002/chem.202000678.

[10] A. Varma, A. S. Mukasyan, A. S. Rogachev, and K. V. Manukyan, "Solution Combustion Synthesis of Nanoscale Materials," *Chem Rev*, vol. 116, no. 23, pp. 14493–14586, Dec. 2016, doi: 10.1021/acs.chemrev.6b00279.

[11] F. Deganello and A. K. Tyagi, "Solution combustion synthesis, energy and environment: Best parameters for better materials," *Progress in Crystal Growth and Characterization of Materials*, vol. 64, no. 2, pp. 23–61, Jun. 2018, doi: 10.1016/j.pcrysgrow.2018.03.001.

[12] A. Khort, J. Hedberg, N. Mei, V. Romanovski, E. Blomberg, and I. Odnevall, "Corrosion and transformation of solution combustion synthesized Co, Ni and CoNi nanoparticles in synthetic freshwater with and without natural organic matter," *Sci Rep*, vol. 11, no. 1, p. 7860, Apr. 2021, doi: 10.1038/s41598-021-87250-7.

[13] F. Deganello, "Nanomaterials for environmental and energy applications prepared by solution combustion based-methodologies: Role of the fuel," *Mater Today Proc*, vol. 4, no. 4, pp. 5507–5516, 2017, doi: 10.1016/j.matpr.2017.06.006.

[14] E. Carlos, R. Branquinho, P. Barquinha, R. Martins, and E. Fortunato, "New strategies toward high-performance and low-temperature processing of solution-based metal oxide TFTs," in *Chemical Solution Synthesis for Materials Design and Thin Film Device Applications*, Elsevier, 2021, pp. 585–621. doi: 10.1016/B978-0-12-819718-9.00003-0.

[15] Y. S. Rim, W. H. Jeong, D. L. Kim, H. S. Lim, K. M. Kim, and H. J. Kim, "Simultaneous modification of pyrolysis and densification for low-temperature solution-processed flexible oxide thin-film transistors," *J Mater Chem*, vol. 22, no. 25, p. 12491, 2012, doi: 10.1039/c2jm16846d.

[16] K. Song, C. Young Koo, T. Jun, D. Lee, Y. Jeong, and J. Moon, "Low-temperature soluble InZnO thin film transistors by microwave annealing," *J Cryst Growth*, vol. 326, no. 1, pp. 23–27, Jul. 2011, doi: 10.1016/j.jcrysgro.2011.01.044.

[17] Y. Jeong *et al.*, "Effects of hydrogen plasma treatment on the electrical behavior of solution-processed ZnO transistors," *J Appl Phys*, vol. 116, no. 7, Aug. 2014, doi: 10.1063/1.4893470.

[18] W. Cho, M. Ahn, and K. Jo, "Performance Enhancement of Solution-Derived Zinc–Tin–Oxide Thin Film Transistors by Low-Temperature Microwave Irradiation," *physica status solidi (a)*, vol. 214, no. 12, Dec. 2017, doi: 10.1002/pssa.201700350.

[19] J. Park *et al.*, "Effective Atmospheric-Pressure Plasma Treatment toward High-Performance Solution-Processed Oxide Thin-Film Transistors," *ACS Appl Mater Interfaces*, vol. 10, no. 36, pp. 30581–30586, Sep. 2018, doi: 10.1021/acsami.8b11111.

[20] H. Kwak *et al.*, "Employment of rapid thermal annealing for solution-processed InGaZnO thin film transistors," *Journal of Materials Science: Materials in Electronics*, vol. 29, no. 10, pp. 8660–8665, May 2018, doi: 10.1007/s10854-018-8880-z.

[21] Y.-H. Kim *et al.*, "Flexible metal-oxide devices made by room-temperature photochemical activation of sol–gel films," *Nature*, vol. 489, no. 7414, pp. 128–132, Sep. 2012, doi: 10.1038/nature11434.

[22] J. Yang, B. Wang, Y. Zhang, X. Ding, and J. Zhang, "Low-temperature combustion synthesis and UV treatment processed p-type Li:$NiO_x$ active semiconductors for high-performance electronics," *J Mater Chem C Mater*, vol. 6, no. 46, pp. 12584–12591, 2018, doi: 10.1039/C8TC04594A.

[23] E. Carlos, R. Branquinho, A. Kiazadeh, P. Barquinha, R. Martins, and E. Fortunato, "UV-Mediated Photochemical Treatment for Low-Temperature Oxide-Based Thin-Film Transistors," *ACS Appl Mater Interfaces*, vol. 8, no. 45, pp. 31100–31108, Nov. 2016, doi: 10.1021/acsami.6b06321.

[24] E. Carlos *et al.*, "Boosting Electrical Performance of High-κ Nanomultilayer Dielectrics and Electronic Devices by Combining Solution Combustion Synthesis and UV Irradiation," *ACS Appl Mater Interfaces*, vol. 9, no. 46, pp. 40428–40437, Nov. 2017, doi: 10.1021/acsami.7b11752.

[25] E. Carlos *et al.*, "Printed, Highly Stable Metal Oxide Thin-Film Transistors with Ultra-Thin High-κ Oxide Dielectric," *Adv Electron Mater*, vol. 6, no. 3, Mar. 2020, doi: 10.1002/aelm.201901071.

[26] W. M. Kim, J.-H. Jeong, and J. K. Park, "Transport characteristics of thermally degraded ZnO films doped with Al," *Current Applied Physics*, vol. 14, no. 5, pp. 691–696, May 2014, doi: 10.1016/j.cap.2014.02.026.

[27] V. R. Buch, A. K. Chawla, and S. K. Rawal, "Review on electrochromic property for WO3 thin films using different deposition techniques," *Mater Today Proc*, vol. 3, no. 6, pp. 1429–1437, 2016, doi: 10.1016/j.matpr.2016.04.025.

# A

# BEST PARAMETERS FILM PROPERTIES

**Table A.1.** Thickness obtained by spectroscopic ellipsometry, electrical properties by Hall effect measurements and transmittance on the visible range of doped indium oxide thin films. All with 0.5 M% Hf dopant, 2-ME solvent and annealed at 300 °C.

| Film conditions | Thickness (nm) | ϱ (Ω·cm) | μ ($cm^2/V·s$) | N ($cm^{-3}$) | $T_{380-750nm}$ (%) |
|---|---|---|---|---|---|
| 2h - IR | 96.1 ± 1 | 1.42 ± 0.24 | 0.86 ± 0.05 | $5.3 \pm 0.9 \times 10^{18}$ | 82 ± 2 |
| 2h - Hotplate | 97.2 ± 0.5 | 4.29 ± 0.72 | 0.43 ± 0.11 | $3.6 \pm 0.9 \times 10^{18}$ | 85 ± 3 |
| 1h - Hotplate + UV | 112.8 ± 0.5 | 25923 ± 25360 | 2.91 ± 0.86 | $5.1 \pm 7.9 \times 10^{14}$ | 86 ± 3 |

**Table A.2.** Thickness obtained by spectroscopic ellipsometry, electrical properties by Hall effect measurements and transmittance on the visible range of doped indium oxide thin films. All 0.5 M% Hf dopant, 2-ME solvent and annealed in an IR oven.

| Film conditions | Thickness (nm) | ϱ (Ω·cm) | μ ($cm^2/V·s$) | N ($cm^{-3}$) | $T_{380-750nm}$ (%) |
|---|---|---|---|---|---|
| 1h - 350 °C | 85.7 ± 1 | 0.5 ± 0.13 | 0.42 ± 0.08 | $3.1 \pm 0.3 \times 10^{19}$ | 81 ± 2 |
| 2h - 350 °C | 87.1 ± 0.9 | 0.13 ± 0.01 | 1.33 ± 0.06 | $3.6 \pm 0.2 \times 10^{19}$ | 81 ± 2 |
| 2h - 250 °C | 93.6 ± 1 | 35.77 ± 10.87 | 0.86 ± 0.17 | $2.2 \pm 0.7 \times 10^{17}$ | |
| 4h - 250 °C | 96.8 ± 1.1 | 77.83 ± 33.86 | 0.51 ± 0.13 | $1.9 \pm 1 \times 10^{17}$ | |

**Table A.3.** Thickness obtained by spectroscopic ellipsometry, electrical properties by Hall effect measurements and transmittance on the visible range of doped indium oxide thin films. All with 2-ME solvent and annealed with a hotplate for 1 h at 400 °C.

| Film conditions | Thickness (nm) | ϱ (Ω·cm) | μ ($cm^2/V·s$) | N ($cm^{-3}$) | $T_{380-750nm}$ (%) |
|---|---|---|---|---|---|
| 0.5 M% Hf | 85.8 ± 0.8 | 0.59 ± 0.14 | 1.95 ± 0.4 | $5.6 \pm 0.2 \times 10^{18}$ | 81 ± 3 |
| 1 M% Zr | 83.2 ± 0.6 | 0.31 ± 0.18 | 1.3 ± 0.34 | $7.1 \pm 2.2 \times 10^{18}$ | 80 ± 2 |

**Table A.4.** Thickness obtained by spectroscopic ellipsometry, electrical properties by Hall effect measurements and transmittance on the visible range of doped indium oxide thin films. All with 2-ME solvent and annealed in an IR oven for 2 h at 350 °C.

| Film conditions | Thickness (nm) | ϱ (Ω·cm) | μ ($cm^2/V·s$) | N ($cm^{-3}$) | $T_{380-750nm}$ (%) |
|---|---|---|---|---|---|
| 0.5 M% Hf | 87.1 ± 0.9 | 0.13 ± 0.01 | 1.33 ± 0.06 | $3.6 \pm 0.2 \times 10^{19}$ | 81 ± 2 |
| 1 M% Zr | 87.8 ± 0.8 | 0.18 ± 0.07 | 1.13 ± 0.29 | $1.3 \pm 0.3 \times 10^{19}$ | 81 ± 2 |

**Table A.5.** Thickness obtained by spectroscopic ellipsometry, electrical properties by Hall effect measurements and transmittance on the visible range of doped indium oxide thin films. All with 2-ME solvent and annealed in an IR oven for 2 h at 300 °C.

| Film conditions | Thickness (nm) | ϱ (Ω·cm) | μ ($cm^2/V·s$) | N ($cm^{-3}$) | $T_{380-750nm}$ (%) |
|---|---|---|---|---|---|
| 0.5 M% Hf | 96.1 ± 1 | 1.42 ± 0.24 | 0.86 ± 0.05 | $5.3 \pm 0.9 \times 10^{18}$ | 82 ± 2 |
| 1 M% Zr | 95 ± 0.4 | 9.37 ± 3.32 | 0.44 ± 0.16 | $6.8 \pm 1.1 \times 10^{17}$ | 82 ± 2 |

**Table A.6.** Thickness obtained by spectroscopic ellipsometry, electrical properties by Hall effect measurements and transmittance on the visible range of doped indium oxide thin films. All with 0.5 M% Hf dopant and annealed in an IR oven for 2 h at 350 °C.

| Film conditions | Thickness (nm) | ϱ (Ω·cm) | μ ($cm^2/V·s$) | N ($cm^{-3}$) | $T_{380-750nm}$ (%) |
|---|---|---|---|---|---|
| 2-ME | 87.1 | 0.13 ± 0.01 | 1.33 ± 0.06 | $3.6 \pm 0.2 \times 10^{19}$ | 81 ± 1 |
| 0.5 M% Hf | 125.2 ± 0.9 | 0.31 ± 0.01 | 4.02 ± 0.59 | $5.1 \pm 0.8 \times 10^{18}$ | 84 ± 4 |
| Ethanol + EG | 117.4 ± 0.6 | 0.74 ± 0.12 | 0.39 ± 0.18 | $2.4 \pm 0.7 \times 10^{19}$ | 86 ± 3 |

# B

# ANNEALING TEMPERATURE EFFECT FULL PROPERTIES

**Table B.1.** Thickness obtained by spectroscopic ellipsometry, electrical properties by Hall effect measurements and transmittance on the visible range of doped indium oxide thin films. All with 0.5 M% Hf dopant, 2-ME solvent and annealed in an IR oven for 2 h.

| Film conditions | Thickness (nm) | ϱ (Ω·cm) | μ ($cm^2/V·s$) | N ($cm^{-3}$) | $T_{380-750nm}$ (%) |
|---|---|---|---|---|---|
| 200 °C | 115.2 ± 0.6 | 530 ± 62.36 | 0.9 ± 0.81 | $2.4 \pm 2.1 \times 10^{16}$ | 85 ± 3 |
| 250 °C | 93.6 ± 1 | 35.77 ± 10.87 | 0.86 ± 0.17 | $2.2 \pm 0.7 \times 10^{17}$ | |
| 300 °C | 96.1 ± 1 | 1.42 ± 0.24 | 0.86 ± 0.05 | $5.3 \pm 0.9 \times 10^{18}$ | 82 ± 2 |
| 350 °C | 87.1 ± 0.9 | 0.13 ± 0.01 | 1.33 ± 0.06 | $3.6 \pm 0.2 \times 10^{19}$ | 81 ± 2 |

**Table B.2.** Thickness obtained by spectroscopic ellipsometry, electrical properties by Hall effect measurements and transmittance on the visible range of doped indium oxide thin films. All with 0.5 M% Hf dopant, 2-ME solvent and annealed with a hotplate for 2 h.

| Film conditions | Thickness (nm) | ϱ (Ω·cm) | μ ($cm^2/V·s$) | N ($cm^{-3}$) | $T_{380-750nm}$ (%) |
|---|---|---|---|---|---|
| 200 °C | 113.4 ± 0.5 | 31.67 ± 2.78 | 0.2 ± 0.09 | $1.2 \pm 0.8 \times 10^{18}$ | 89 ± 2 |
| 250 °C | 100.2 ± 1.4 | 80.87 ± 13.24 | 0.32 ± 0.28 | $3.6 \pm 2.1 \times 10^{17}$ | 86 ± 3 |
| 300 °C | 97.2 ± 0.5 | 4.29 ± 0.72 | 0.43 ± 0.11 | $3.6 \pm 0.9 \times 10^{18}$ | 85 ± 3 |
| 350 °C | 87.4 ± 0.8 | 0.73 ± 0.14 | 1.24 ± 0.03 | $7 \pm 1.4 \times 10^{18}$ | 82 ± 2 |

**Table B.3.** Thickness obtained by spectroscopic ellipsometry, electrical properties by Hall effect measurements and transmittance on the visible range of doped indium oxide thin films. All with 0.5 M% Hf dopant, MP solvent and annealed in an IR oven for 2 h.

| Film conditions | Thickness (nm) | ϱ (Ω·cm) | μ ($cm^2/V·s$) | N ($cm^{-3}$) | $T_{380-750nm}$ (%) |
|---|---|---|---|---|---|
| 200 °C | 150.1 ± 0.8 | 1520 ± 113.14 | 2.06 ± 2.52 | $8.3 \pm 10.3 \times 10^{15}$ | 88 ± 3 |
| 250 °C | 138.3 ± 1.4 | 18.13 ± 5.69 | 1.53 ± 1.14 | $7.3 \pm 10.1 \times 10^{17}$ | 87 ± 4 |
| 300 °C | 126.1 ± 1.3 | 2.37 ± 0.5 | 0.78 ± 0.06 | $3.5 \pm 0.6 \times 10^{18}$ | 86 ± 4 |
| 350 °C | 125.2 ± 0.9 | 0.31 ± 0.01 | 4.02 ± 0.59 | $5.1 \pm 0.8 \times 10^{18}$ | 84 ± 4 |

**Table B.4.** Thickness obtained by spectroscopic ellipsometry, electrical properties by Hall effect measurements and transmittance on the visible range of doped indium oxide thin films. All with 0.5 M% Hf dopant, MP solvent and annealed with a hotplate for 2 h.

| Film conditions | Thickness (nm) | ϱ (Ω·cm) | μ ($cm^2/V·s$) | N ($cm^{-3}$) | $T_{380-750nm}$ (%) |
|---|---|---|---|---|---|
| 200 °C | 134.2 ± 0.8 | 16 ± 4.2 | 0.17 ± 0.09 | $3 \pm 1.6 \times 10^{18}$ | 90 ± 4 |
| 250 °C | 127.3 ± 1.1 | 82.47 ± 25.58 | 0.34 ± 0.21 | $2.7 \pm 1 \times 10^{17}$ | 88 ± 3 |
| 300 °C | 118 ± 1.4 | 9.78 ± 1.72 | 0.62 ± 0.16 | $1.2 \pm 0.6 \times 10^{18}$ | 88 ± 3 |
| 350 °C | 109.3 ± 0.6 | 0.56 ± 0.14 | 1.34 ± 0.24 | $0.9 \pm 0.2 \times 10^{19}$ | 86 ± 4 |

# C

# Optical Characterization Graphs

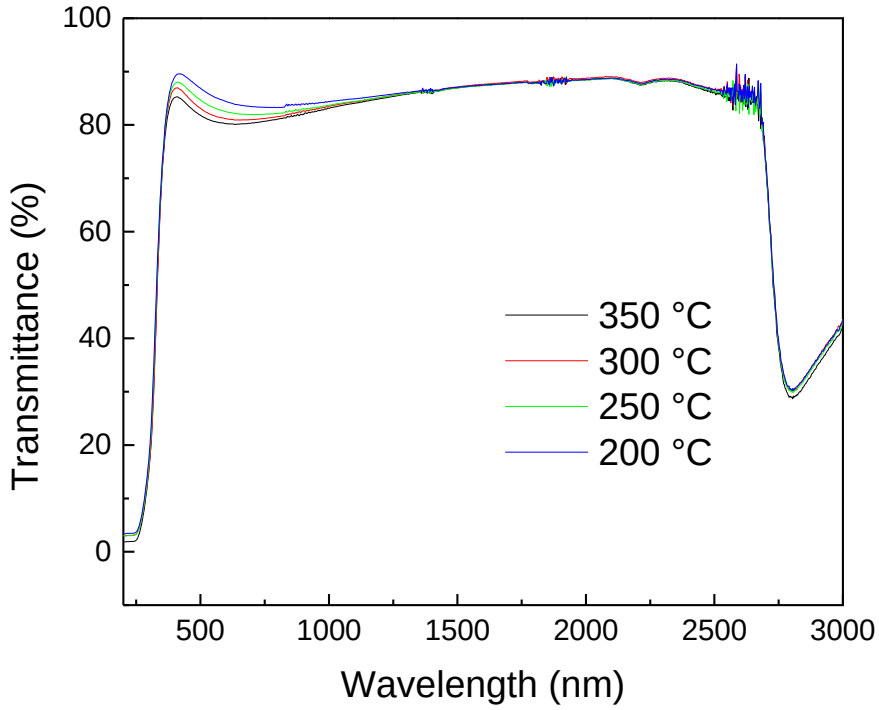


**Figure C.1.** Transmittance spectra of indium oxide thin films with 2-ME as the solvent and IR as the annealing method.

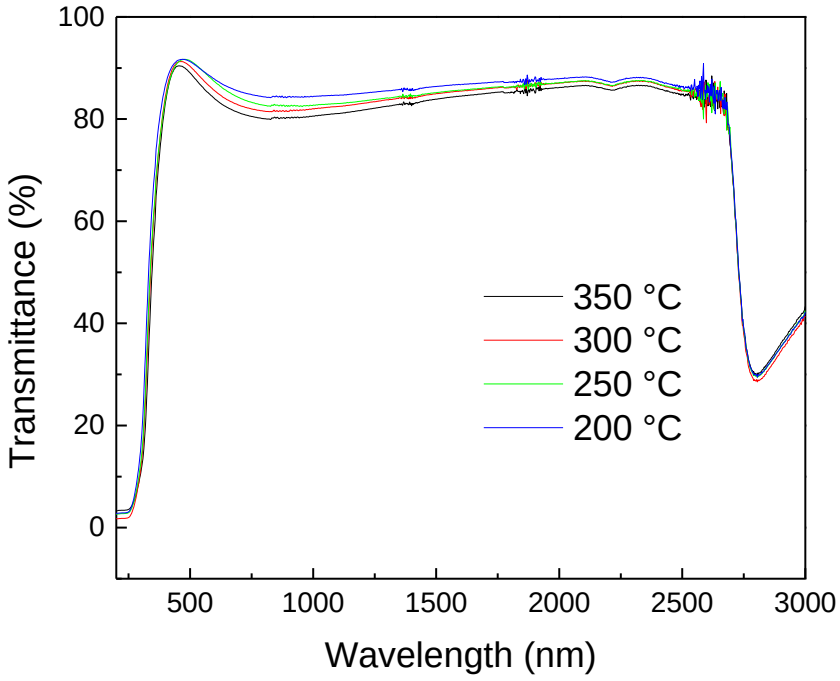


**Figure C.2.** Transmittance spectra of indium oxide thin films with MP as the solvent and IR as the annealing method.

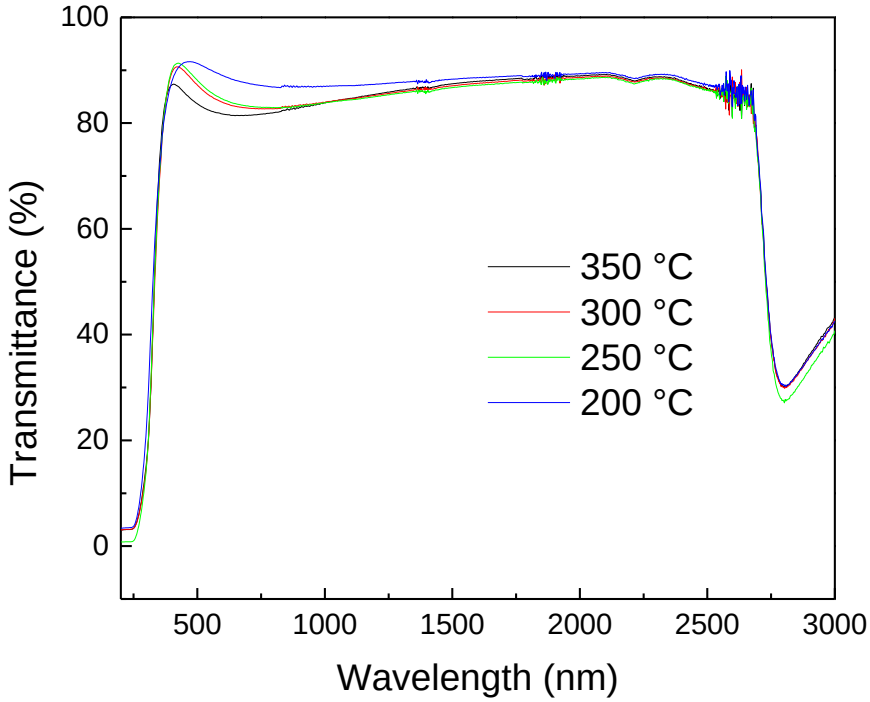


**Figure C.3.** Transmittance spectra of indium oxide thin films with 2-ME as the solvent and hotplate as the annealing method.

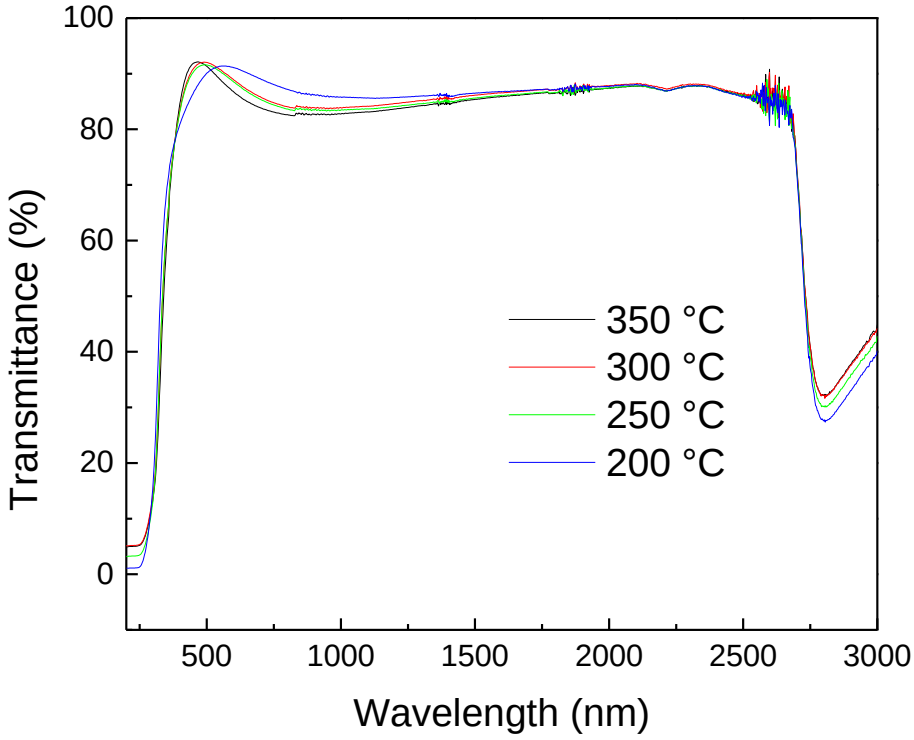


**Figure C.4.** Transmittance spectra of indium oxide thin films with MP as the solvent and hotplate as the annealing method.